Journal of Southeast University (English Edition) Vol. 38, No. 3, pp. 235 - 241 Sept. 2022 ISSN 1003—7985

# Temperature prediction model for a high-speed motorized spindle based on back-propagation neural network optimized by adaptive particle swarm optimization

Lei Chunli Zhao Mingqi Liu Kai Song Ruizhe Zhang Huqiang

(School of Mechanical and Electrical Engineering, Lanzhou University of Technology, Lanzhou 730050, China)

**Abstract:** To predict the temperature of a motorized spindle more accurately, a novel temperature prediction model based on the back-propagation neural network optimized by adaptive particle swarm optimization (APSO-BPNN) is proposed. First, on the basis of the PSO-BPNN algorithm, the adaptive inertia weight is introduced to make the weight change with the fitness of the particle, the adaptive learning factor is used to obtain different search abilities in the early and later stages of the algorithm, the mutation operator is incorporated to increase the diversity of the population and avoid premature convergence, and the APSO-BPNN model is constructed. Then, the temperature of different measurement points of the motorized spindle is forecasted by the BPNN, PSO-BPNN, and APSO-BPNN models. The experimental results demonstrate that the APSO-BPNN model has a significant advantage over the other two methods regarding prediction precision and robustness. The presented algorithm can provide a theoretical basis for intelligently controlling temperature and developing an early warning system for high-speed motorized spindles and machine tools.

**Key words:** temperature prediction; high-speed motorized spindle; particle swarm optimization algorithm; back-propagation neural network; robustness

**DOI:** 10.3969/j.issn.1003-7985.2022.03.004

High-speed computer numerical control (CNC) machine tools are the technical foundation of the equipment manufacturing industry. As the core component of CNC machine tools, the technology and performance of the motorized spindle unit affect machine tool development. As a highly integrated spindle, the power loss of the motor and the friction heat of the bearing of a motorized spindle are the main heat sources. The thermal character directly affects the machining accuracy and service life of motorized spindles and machine tools[1]. According to statistics, the error caused by the thermal deformation of machine tools accounts for 40% to 70% of the total manufacturing error in precision machining[2]. The temperature increase is an important index for evaluating the high-speed operation of motorized spindles[3-5]. Therefore, developing motorized spindles inevitably requires accurate prediction and control of the temperature increase and thermal deformation to realize the automation and intelligence of motorized spindles[6-7]. However, because the thermal structure of spindles has complex boundary conditions and joint surfaces, large errors are obtained in the theoretical modeling and finite element analysis of their thermal design[8]. Temperature prediction is difficult because the temperature of the internal parts of a motorized spindle is not easy to obtain directly, and the temperature distribution of a motorized spindle is nonlinear and complex, resulting in the low accuracy of the predicted temperature. Therefore, the temperature increase characteristics of spindles must be obtained through a thermal balance test, and the model parameters must be checked. Zhang et al.[9] proposed a prediction model of temperature increase in high-speed and precision motorized spindles, which was combined with the calculated results of the finite element model and test data to accurately predict the temperature field of a motorized spindle under different working conditions. A comprehensive prediction model was applied to forecast the thermal-mechanical behavior of a spindle-bearing system considering various bearing surroundings[10]. Liu et al.[11] introduced a BP neural network for the thermal error prediction of a five-axis machining center. Jian et al.[12] predicted spindle thermal deformation using the BPNN. Kumar et al.[13] presented a hybrid model based on particle swarm optimization (PSO) and an emerging extreme learning machine to forecast the temperature. The BP neural network based on the PSO algorithm was applied to predict the high-speed grinding temperature of titanium matrix composites[14]. Li et al.[15] established the spindle thermal error prediction model based on the improved PSO (IPSO)-BP neural network, and IPSO was used to optimize the parameters of the BPNN based on the genetic algorithm (GA). An adaptive neuro-fuzzy inference system was used to design two thermal prediction models for

**Received** 2022-01-17, **Revised** 2022-05-25.

**Biography:** Lei Chunli (1977—), female, doctor, associate professor, lclyq2004@163.com.

**Foundation items:** The National Natural Science Foundation of China (No. 51465035), the Natural Science Foundation of Gansu, China (No. 20JR5R-A466).

**Citation:** Lei Chunli, Zhao Mingqi, Liu Kai, et al. Temperature prediction model for a high-speed motorized spindle based on back-propagation neural network optimized by adaptive particle swarm optimization[J]. Journal of Southeast University (English Edition), 2022, 38(3): 235 - 241. DOI: 10.3969/j.issn.1003-7985.2022.03.004.

thermal error compensation in machine tools[16]. These models have high accuracy in predicting a temperature increase or thermal error. However, the above mentioned neuro network models still have deficiencies, such as a lack of population diversity and an inadequate design of learning factors, weights, and other parameters.

In this paper, a BP neural network model based on the adaptive PSO (APSO-BPNN) algorithm is presented to forecast the temperature increase of a motorized spindle. To improve the generalization ability and prediction accuracy of the APSO-BPNN algorithm, the key parameters of the PSO algorithm, the inertia weight and learning factor, are optimized, and the mutation operator is integrated to enhance the diversity of the population and improve the success rate of the optimization. Further, the prediction performance of the BP model, PSO-BPNN model, and APSO-BPNN model are compared, and the results show that the APSO-BPNN model has the best prediction accuracy and generalization ability.

## 1 Modeling Methods for Temperature Prediction of a Motorized Spindle

### 1.1 Basic BP neural network model

BPNNs are trained according to the error back-propagation algorithm, and they have been applied in many fields because of their parallel processing ability, fault tolerance ability, and nonlinear mapping. According to Kolmogorov's theorem[17], a three-layer BPNN can approach any nonlinear function in theory. The main characteristics of a BP network are signal forward transmission and error back-propagation. Therefore, a BPNN can be used to establish the nonlinear mapping relationship between the temperature of motorized spindle parts and time, ambient temperature, and coolant temperature, and the node of the output layer is the temperature of the front bearing outer ring, the temperature of the rear bearing seat, and the temperature of the stator end.

The node number in hidden layer neurons is determined by

$$l = \sqrt{m' + n'} + a' \tag{1}$$

where $m'$ and $n'$ are the numbers of nodes in the input and output layers, respectively, and $a'$ is a constant within $[1, 10]$.

According to Eq. (1), the node number in a hidden layer is determined to be 8 by experiments in this paper. The number of iterations is 100, the learning rate is 0.1, and the target error value is $1.0 \times 10^{-4}$. The transfer functions of the hidden layer and the output layer neurons are tangent S-type transfer functions (Tansig) and linear transfer functions (purelin), respectively. Trainlm is used for network training. Therefore, the structure of the BP network is determined as 3-8-1.

### 1.2 BP model based on the particle swarm optimization algorithm

Although the steepest descent method is adopted in the BP network algorithm, it has problems such as a slow convergence speed and low calculation accuracy, and it easily falls into a local minimum value. However, the PSO algorithm is a swarm intelligence algorithm based on population. It can realize the optimization search through the cooperation and competition between particles to avoid falling into a local optimum. PSO has a higher convergence speed and global optimization ability. Therefore, the PSO algorithm is adopted in this paper to optimize the weights and thresholds of the BP network.

In the PSO algorithm, the particles search in the solution space by following the current optimal particle. The PSO data are initialized as a group of random particles, and then the optimal solution is found through an iteration method. In each iteration, the particle velocity is adjusted based on individual and global extrema, which are composed of an inertial part, cognitive part, and social part. When each particle finds an optimal value, it updates its own speed and position using the following equations[18]:

$$v_{id}^{t+1} = \omega v_{id}^{t} + c_1 r_1 (p_{best\_id} - p_{id}^{t}) + c_2 r_2 (g_{best\_id} - p_{id}^{t}) \tag{2}$$

$$p_{id}^{t+1} = p_{id}^{t} + v_{id}^{t+1} \tag{3}$$

where $v_{id}$ and $p_{id}$ are the velocity and position of the $i$-th particle in the $d$-th generation, respectively; $t$ is the number of iterations; $\omega$ is the inertia weight; $c_1$ is called the cognitive learning factor; $c_2$ is the social learning factor; $r_1$ and $r_2$ are two uniformly distributed random numbers independently generated within $[0, 1]$[19], and $p_{best\_id}$ and $g_{best\_id}$ are the individual and the swarm historical best solutions at the $d$-th generation.

### 1.3 BP model based on the adaptive particle swarm optimization algorithm

The BP algorithm optimized by PSO still has disadvantages, such as low search accuracy and easy premature convergence, which reduces the predictive accuracy. This result is mainly due to the phenomenon of particle convergence and the decrease in population diversity. Therefore, a BP neural network based on the adaptive particle swarm optimization (APSO-BPNN) algorithm is proposed, which improves the inertia weight and learning factor of the PSO-BP algorithm and integrates the mutation operator of the GA to improve the prediction precision.

#### 1.3.1 Adaptive inertia weight

The inertia weight of a particle describes its ability to maintain the previous motion state. In the early experiments, it was set to a fixed value within $[0.2, 1.2]$. In fact, the inertia weight decreases not only with increasing iteration times but also with decreasing distance from the

global optimum. When the inertia weight is reduced, the local optimization ability of the algorithm can be enhanced. When the inertia weight is increased, the global search ability of the algorithm can be increased. Therefore, the adaptive nonlinear dynamic inertia weight can avoid the algorithm falling into a local optimum and improve the search efficiency. When the fitness value of a particle is dispersed, the inertia weight decreases. When the fitness value is near the local optimal solution, the inertia weight increases. The calculation formula is shown as follows:

$$\omega = \begin{cases} \omega_{\min} - \dfrac{(\omega_{\max} - \omega_{\min})(f - f_{\min})}{f_{\text{avg}} - f_{\min}} & f \leqslant f_{\text{avg}} \\ \omega_{\max} & f > f_{\text{avg}} \end{cases} \quad (4)$$

where $\omega_{\max}$ and $\omega_{\min}$ are the maximum and minimum values of the inertia weight, respectively; $f$ is the fitness value of the particle; $f_{\text{avg}}$ is the average fitness value; $f_{\min}$ is the minimum fitness value.

### 1.3.2 Adaptive learning factor

Generally, the learning factors $c_1$ and $c_2$ are set as fixed values in the PSO algorithm, and the self-learning ability and social learning ability of particles are considered equal. However, the search ability of particles in the early and later stages is easily affected by $c_1$ and $c_2$. Therefore, to search in global space, an adaptive learning factor formula is proposed in this paper.

In the initial search stage of the PSO algorithm, $c_1$ is set to a larger value and $c_2$ is set to a smaller value, which makes the particles learn toward the optimal value, promotes the particles to obtain the best position in their history, and improves the local search ability of particles. In the later stage of the PSO algorithm, $c_1$ takes a smaller value and $c_2$ takes a larger value so that the particles tend to the global optimum to enhance the global search ability and the convergence speed. The improved formulas of $c_1$ and $c_2$ are presented as follows:

$$c_1 = 0.95c_{\max 1} + (c_{\min 1} - c_{\max 1})\frac{g}{G_{\max}} \quad (5)$$

$$c_2 = 0.95c_{\max 2} + (c_{\min 2} - c_{\max 2})\frac{g}{G_{\max}} \quad (6)$$

where $c_{\max}$ and $c_{\min}$ are the maximum and minimum learning factors, respectively; $g$ is the current iteration number; $G_{\max}$ is the maximum number of evolutions.

### 1.3.3 Adaptive mutation operator

The GA is a computational model used to simulate the biological evolutionary mechanism of nature proposed by Holland[20]. The mutation operator can increase local random search ability and accelerate the convergence speed of the algorithm to the optimal solution. In addition, it can effectively increase the diversity of the population and prevent premature convergence. Therefore, the mutation operator is introduced into the PSO-BPNN algorithm. When the mutation operator is used, particles are reinitialized with a certain probability after each update to increase the disturbance of the algorithm and prevent it from falling into a local minimum. At the same time, the mutation operator is embedded in the PSO-BPNN algorithm to expand the population space reduced in the iterative process and search in a larger space to realize the adaptive adjustment of the operator and improve the accuracy of prediction.

The $j$-th gene of the $i$-th individual is mutated as[21]

$$a_{ij} = \begin{cases} a_{ij} + (a_{ij} - a_{\max})f(g) & r > 0.5 \\ a_{ij} + (a_{\min} - a_{ij})f(g) & r \leqslant 0.5 \end{cases} \quad (7)$$

where $a_{\max}$ and $a_{\min}$ are the maximum and minimum bounds of gene $a_{ij}$; $r$ is a random number within $[0, 1]$.

$$f(g) = r_2\left(1 - \frac{g}{G_{\max}}\right)^2 \quad (8)$$

where $r_2$ is a random number.

### 1.3.4 Calculation process of the back-propagation neural network optimized by adaptive particle swarm optimization model

On the basis of the PSO-BPNN algorithm, the adaptive inertia weight, adaptive learning factor, and adaptive mutation operator are introduced in the APSO-BPNN algorithm. The detailed procedure of the APSO-BPNN model is summarized as follows:

**Step 1** Initialize the parameters of the particle swarm, including the number of iterations, population size, maximum and minimum velocities, and maximum and minimum positions. In this paper, $t$ is initialized to 100, the population size is 30, $v$ is within $[-5, 5]$, $p$ is within $[-10, 10]$, $c_1$ is within $[0.8, 2.4]$, $c_2$ is within $[2.4, 0.8]$, and $\omega$ is within $[0.4, 0.9]$.

**Step 2** Substitute the initial weights and thresholds of the BP neural network into the PSO algorithm to initialize the particle velocities and positions and calculate the fitness value of the particle using

$$f = k'\left[\sum_{i=1}^{n} \text{abs}(y_i - o_i)\right] \quad (9)$$

where $k'$ is a coefficient; $n$ is the training sample number of the BP neural network; $y_i$ is the actual output of the $i$-th node; $o_i$ is the predicted output of the $i$-th node.

**Step 3** Compare the individual extremum $p_{\text{id}}$ and global extremum $g_{\text{id}}$ with the fitness value. If $f > p_{\text{id}}$, $p_{\text{id}}$ will be replaced by $f$; if $f > g_{\text{id}}$, $g_{\text{id}}$ will be replaced by $f$.

**Step 4** Solve the adaptive inertia weight according to Eq. (4).

**Step 5** Solve the adaptive learning factors according to Eqs. (5) and (6).

**Step 6** Substitute the results of Steps 4 and 5 into Eqs. (2) and (3) and update the velocities and positions of the particles according to Eqs. (2) and (3), then update the fitness value of the particle.

**Step 7** Carry out the mutation operation on the particles according to Eqs. (7) and (8) and update the individual and global extremum of the particle.

**Step 8** Judge whether the termination condition is reached. If so, the optimized weight and threshold are substituted into BP neural network training. Otherwise, return to Step 4 to continue iterating.

**Step 9** Judge whether the error between the predicted value and the actual value after training meets the termination condition. If so, the iteration will be suspended, and the prediction result will be outputted. Otherwise, return to Step 8 to retrain until the result outputs.

## 2 Temperature Experiments

On the basis of the test rig of a motorized spindle built by the research team, the thermocouple was embedded in the motorized spindle, and the temperatures of the front bearing outer ring, the rear bearing seat, and the stator end were measured. The temperature measuring points of the motorized spindle are shown in Fig. 1.

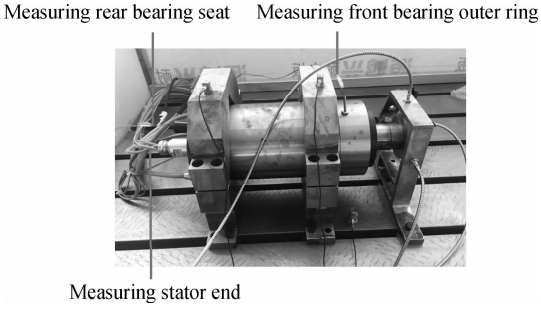


**Fig. 1** Temperature measurement points of a motorized spindle

The temperature values at three test points, the ambient temperature, and the coolant temperature of the motorized spindle at 12 000 r/min were measured. A set of data was collected every 15 s to ensure that the temperature of the motorized spindle could be recorded in detail until its running reached a steady state at this speed. A total of 340 groups of data samples were obtained after the preliminary processing of the experimental data. The temperature curves at this speed are drawn, as shown in Fig. 2. Fig. 2 shows that the motorized spindle reaches thermal balance at approximately 5 100 s. A nonlinear relationship between temperature and time is also apparent at the three

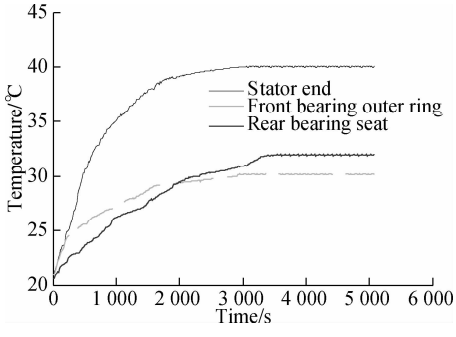


**Fig. 2** Temperature values of measuring points at 12 000 r/min

measuring points. Therefore, using BPNN to establish the relationship between spindle temperature and time, coolant temperature, and ambient temperature is reasonable.

## 3 Temperature Prediction of a Motorized Spindle

When the motorized spindle rotates at high speed, the change in its internal temperature has strong nonlinear characteristics, and an excessive temperature increase will affect the machining accuracy of the spindle and the machine tool. The temperature prediction of the spindle is of great significance for exploring the trend of temperature increase and providing effective control decisions. Therefore, the BPNN, PSO-BPNN, and APSO-BPNN algorithms are applied to the temperature prediction of the motorized spindle in this paper. All the experiments are carried out on the same machine with a 2.10 GHz Core 2 Duo CPU, 64 GB memory, and Windows 10 operating system.

### 3.1 Data processing

The 340 groups of experimental data are divided into two parts. First, the data are numbered; then, according to the method of sequential extraction, 1 group is taken out from every 5 groups, and 68 groups are obtained and considered testing samples. Second, the remaining data are arranged in order to form 272 groups for training samples. To eliminate the difference in the order of magnitude among all dimensional data, the data are processed using the data normalization method and transformed into a number within [0, 1]. The maximum/minimum method is adopted in this paper. The formula is[22]

$$T'_k = \frac{T_k - T_{\min}}{T_{\max} - T_{\min}} \tag{10}$$

where $T_{\min}$ and $T_{\max}$ are the minimum and maximum values in the data sequence, respectively; and $T_k$ is the temperature value at time $k$.

### 3.2 Temperature prediction and discussion

On the basis of the BPNN, PSO-BPNN, and APSO-BPNN models, the temperature increase in the three measurement points of the motorized spindle is predicted. The temperature increase of the front bearing is analyzed in detail, and the result is shown in Fig. 3.

Figs. 3 (a), (c) and (e) show that the predicted values of the APSO-BPNN model for the front bearing outer ring are in the best agreement with the actual values, and the temperature fluctuation is also finely predicted. From Figs. 3 (b), (d) and (f), the temperature prediction errors based on the BPNN model, the PSO-BPNN model, and the APSO-BPNN model are distributed from −0.43 to 0.49 ℃, −0.15 to 0.32 ℃, and −0.18 to 0.15 ℃,

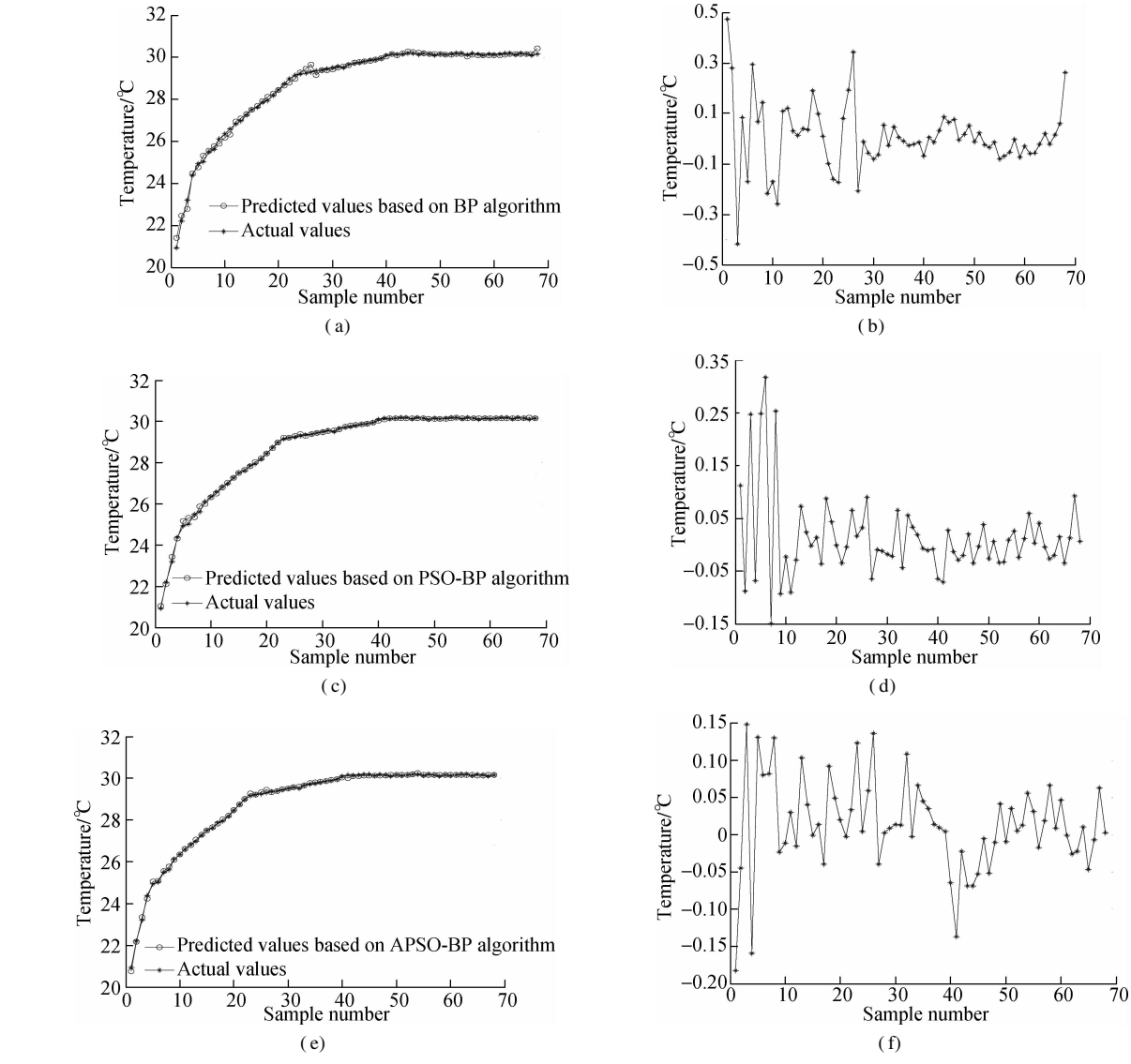


**Fig. 3** Prediction temperature and prediction errors of the outer ring of the front bearing by three algorithms. (a) Predicted value based on the BP algorithm; (b) Prediction error based on the BP algorithm; (c) Predicted value based on the PSO-BP algorithm; (d) Prediction error based on the PSO-BP algorithm; (e) Predicted value based on the APSO-BP algorithm; (f) Prediction error based on the APSO-BP algorithm

respectively. The APSO-BPNN model has the smallest errors and the highest prediction accuracy among the three models.

With the same approach, the prediction temperature and prediction error of the rear bearing seat are calculated using the three models. The temperature prediction errors based on the BP model, PSO-BP model, and APSO-BP model are distributed from −0.3 to 0.5 ℃, −0.2 to 0.25 ℃, and −0.1 to 0.2 ℃, respectively. Additionally, the prediction temperature and prediction error of the stator end by the three models are also calculated. The temperature prediction errors based on the three models are distributed from −0.4 to 0.6 ℃, −0.3 to 0.4 ℃, and −0.25 to 0.2 ℃, respectively. Therefore, it can be concluded that the prediction errors of the three temperature points forecasted by APSO-BPNN are the smallest, which proves that the APSO-BPNN model has a stronger generalization ability and higher predictive precision than the comparison algorithms.

To evaluate the prediction results more intuitively, the mean square error (MSE) function, mean absolute error (MAE) function, and $R$-squared are introduced. The MSE between the experimental data and prediction data is used to evaluate the change degree of data. The smaller the MSE value is, the higher the prediction accuracy of the model is. The MAE is used to reflect the actual situation of the prediction error. $R^2$ is used to reflect the fitting effect of the model. The larger the value of $R^2$, the better the fitting effect of the model. The calculation formulas are shown as[23]

$$\mathrm{MSE} = \frac{1}{N}\sum_{i=1}^{N}(y_i - o_i)^2 \tag{11}$$

$$\mathrm{MAE} = \frac{1}{N}\sum_{i=1}^{N}|(y_i - o_i)| \tag{12}$$

$$R^2 = 1 - \frac{\sum_{i=1}^{N} (y_i - o_i)^2}{\sum_{i=1}^{N} (y_i - \bar{y})^2} \tag{13}$$

The values of MSE, MAE, and $R^2$ by using the BP-NN, PSO-BPNN, and APSO-BPNN algorithms are calculated. The calculation results are shown in Tab. 1.

Tab. 1 shows that the MSE and MAE values of the APSO-BPNN model are the smallest among the three models, while the $R^2$ value of the APSO-BPNN model is the highest, which indicates that the APSO-BPNN model has the highest prediction accuracy and the best fitting effect.

**Tab. 1** Evaluation of prediction models

| Evaluating indicator | Prediction model | Front bearing outer ring | Rear bearing seat | Stator end |
|---|---|---|---|---|
| MSE | BPNN | 0.018 6 | 0.019 9 | 0.016 5 |
| | PSO-BPNN | 0.011 3 | 0.010 6 | 0.011 9 |
| | APSO-BPNN | 0.006 4 | 0.005 7 | 0.007 2 |
| MAE | BPNN | 0.091 9 | 0.108 7 | 0.081 5 |
| | PSO-BPNN | 0.071 3 | 0.059 0 | 0.066 7 |
| | APSO-BPNN | 0.050 3 | 0.051 9 | 0.057 9 |
| $R^2$ | BPNN | 0.995 9 | 0.998 2 | 0.998 5 |
| | POS-BPNN | 0.998 6 | 0.999 1 | 0.999 3 |
| | APSO-BPNN | 0.999 4 | 0.999 5 | 0.999 6 |

## 4 Conclusions

1) The proposed temperature prediction model for a motorized spindle based on APSO-BPNN has a better prediction precision and generalization ability than those of the BPNN and PSO-BPNN models.

2) The adaptive inertia weight, the adaptive learning factor, and the mutation operator are integrated into the presented method, which improves the predictive accuracy of the method.

3) The proposed model has high prediction accuracy. However, how to feed back the prediction value to the existing control system for adjusting the parameters of the cooling and lubrication systems or early warning is future research work.

## References


[1] Mayr J, Jedrzejewski J, Uhlmann E, et al. Thermal issues in machine tools[J]. *CIRP Annals*, 2012, **61**(2): 771 − 791. DOI: 10.1016/ j. cirp. 2012. 05.008.

[2] Bryan J. International status of thermal error research (1990)[J]. *CIRP Annals*, 1990, **39**(2): 645 − 656. DOI: 10.1016/s0007-8506(07)63001-7.

[3] Abele E, Altintas Y, Brecher C. Machine tool spindle units[J]. *CIRP Annals*, 2010, **59**(2): 781 − 802. DOI: 10.1016/j. cirp. 2010. 05. 002.

[4] Zhang Y, Wang L F, Zhang Y D, et al. Design and thermal characteristic analysis of motorized spindle cooling system[J]. *Advances in Mechanical Engineering*, 2021, **13** (5): 168781402110208. DOI: 10. 1177/16878140211020878.

[5] Li X H, Liu J Y, Li C, et al. Research on the influence of air-gap eccentricity on the temperature field of a motorized spindle[J]. *Mechanical Sciences*, 2021, **12**(1): 109 − 122. DOI: 10.5194/ms-12-109-2021.

[6] Lee J H, Yang S H. Statistical optimization and assessment of a thermal error model for CNC machine tools[J]. *International Journal of Machine Tools and Manufacture*, 2002, **42**(1): 147 − 155. DOI: 10.1016/S0890-6955(01)00110-9.

[7] Gao Q, Lu L H, Zhang R, et al. Investigation on the thermal behavior of an aerostatic spindle system considering multi-physics coupling effect[J]. *The International Journal of Advanced Manufacturing Technology*, 2019, **102**(9/10/11/12): 3813 − 3823. DOI: 10. 1007/s00170-019-03509-4.

[8] Feng G, Xia C H, Sun L, et al. Fast identification of machine tool spindle temperature rise characteristics based on nonlinear prediction[J]. *Transactions of the Chinese Society for Agricultural Machinery*, 2015, **46**(6): 341 − 348. DOI: 10. 6041/j. issn. 1000-1298. 2015. 06. 049. (in Chinese)

[9] Zhang L X, Li C Q, Li J P, et al. The temperature prediction mode of high speed and high precision motorized spindle[J]. *Journal of Mechanical Engineering*, 2017, **53**(23): 129 − 136. DOI: 10. 3901/JME. 2017. 23. 129. (in Chinese)

[10] Kim S M, Lee S K. Prediction of thermo-elastic behavior in a spindle-bearing system considering bearing surroundings[J]. *International Journal of Machine Tools and Manufacture*, 2001, **41**(6): 809 − 831. DOI: 10.1016/S0890-6955(00)00103-6.

[11] Liu Y, Wang X F, Zhu X G, et al. Thermal error prediction of motorized spindle for five-axis machining center based on analytical modeling and BP neural network[J]. *Journal of Mechanical Science and Technology*, 2021, **35**(1): 281 − 292. DOI: 10.1007/s12206-020-1228-7.

[12] Jian B L, Guo Y S, Hu C H, et al. Prediction of spindle thermal deformation and displacement using back propagation neural network[J]. *Sensors and Materials*, 2020, **32**(1): 431. DOI: 10.18494/sam. 2020. 2606.

[13] Kumar S, Pal S K, Singh R. A novel hybrid model based on particle swarm optimisation and extreme learning machine for short-term temperature prediction using ambient sensors[J]. *Sustainable Cities and Society*, 2019, **49**: 101601. DOI: 10.1016/j. scs. 2019. 101601.

[14] Liu C J, Ding W F, Li Z, et al. Prediction of high-speed grinding temperature of titanium matrix composites using BP neural network based on PSO algorithm[J]. *The International Journal of Advanced Manufacturing Technology*, 2017, **89** (5/6/7/8): 2277 − 2285. DOI: 10. 1007/s00170-016-9267-z.

[15] Li B, Tian X T, Zhang M. Thermal error modeling of machine tool spindle based on the improved algorithm optimized BP neural network[J]. *The International Journal of Advanced Manufacturing Technology*, 2019, **105**(1/2/3/4): 1497 − 1505. DOI: 10.1007/s00170-019-04375-w.

[16] Abdulshahed A M, Longstaff A P, Fletcher S. The application of ANFIS prediction models for thermal error compensation on CNC machine tools[J]. *Applied Soft Compu-*

ting, 2015, **27**: 158 – 168. DOI: 10. 1016/j. asoc. 2014. 11. 012.

[17] Kůrková V. Kolmogorov's theorem and multilayer neural networks[J]. *Neural Networks*, 1992, **5**(3): 501 – 506. DOI: 10. 1016/0893-6080(92)90012-8.

[18] Cui Q L, Li Q Y, Li G Y, et al. Globally-optimal prediction-based adaptive mutation particle swarm optimization[J]. *Information Sciences*, 2017, **418/419**: 186 – 217. DOI: 10. 1016/j. ins. 2017. 07. 038.

[19] Kennedy J, Eberhart R. Particle swarm optimization [C]//*Proceedings of ICNN' 95—International Conference on Neural Networks*. Perth, WA, Australia, 1995: 1942 – 1948. DOI: 10. 1109/ICNN. 1995. 488968.

[20] Holland J. *Adaptation in natural and artificial systems* [M]. Michigan: The University of Michigan Press, 1975: 42 – 56.

[21] Ding F J, Jia X D, Hong T J, et al. Flow stress prediction model of 6061 aluminum alloy sheet based on GA-BP and PSO-BP neural networks [J]. *Rare Metal Materials and Engineering*, 2020, **49**(6): 1840 – 1853. (in Chinese)

[22] Niu H T. Smart safety early warning model of landslide geological hazard based on BP neural network[J]. *Safety Science*, 2020, **123**: 104572. DOI: 10. 1016/j. ssci. 2019. 104572.

[23] Zhang L, Zhang X G, Chen H, et al. A robust temperature prediction model of shuttle kiln based on ensemble random vector functional link network [J]. *Applied Thermal Engineering*, 2019, **150**: 99 – 110. DOI: 10. 1016 / j. applthermaleng. 2018. 12. 092.

# 基于自适应粒子群优化 BP 神经网络的高速电主轴温度预测模型

雷春丽　赵明齐　刘　凯　宋瑞哲　张护强

(兰州理工大学机电工程学院,兰州 730050)

**摘要:**为精确地预测电主轴高速运转时内部温升的变化情况,提出了一种基于自适应粒子群优化 BP 神经网络的电主轴温度预测模型(APSO-BPNN). 该模型在 PSO-BPNN 算法的基础上,引入自适应惯性权重,使权重跟随粒子适应度的变化而变化;采用自适应学习因子,在算法的初期和后期获得不同的搜索能力;融入变异算子,增加种群的多样性,避免算法的早熟收敛等缺点. 然后,分别采用 BPNN、PSO-BPNN 和 APSO-BPNN 预测模型对电主轴不同测温点的温度进行预测. 实验结果表明,与传统的 BP 神经网络和 PSO-BPNN 预测方法相比,所提 APSO-BPNN 模型预测精度最高,鲁棒性最强,可为电主轴及机床温升的智能控制和早期预警系统开发提供理论依据.

**关键词:**温度预测; 高速电主轴; 粒子群优化算法; BP 神经网络; 鲁棒性

**中图分类号:**TH-39